2008 IEEE International Conference on
Robotics and Automation
Pasadena, CA, USA, May 19-23, 2008

Improving the pose accuracy of a planar 3RRR parallel manipulator using kinematic redundancy and optimized switching patterns

Jens Kotlarski, Houssem Abdellatif, and Bodo Heimann

Abstract— **In the present paper kinematic redundancy is proposed in order to improve the achievable pose accuracy of a parallel robot's traveling platform. An additional prismatic actuator is applied to a 3RRR planar parallel manipulator. It allows a selective reconfiguration of the kinematic structure according to several optimization criteria. Based on an index that we denote the *gain* of the Jacobian matrix the position of the redundant actuator is changed in a discrete manner. The resulting optimized *switching patterns* lead to a great increase of the traveling platform's pose accuracy. Between two switching operations the prismatic actuator's position is supposed to be locked. Hence, sources of error, e.g. the joint clearance, can be minimized. Several analysis examples demonstrate the effectiveness of the proposed concept in combination with the developed optimization procedure.**

I. Introduction

Amongst others, one advantage of parallel manipulators in comparison to classical serial manipulators is a higher pose accuracy. The achievable accuracy of parallel manipulators was studied in [1], [2]. In [3] it is mentioned that the achievable accuracy is greatly affected by the manipulator's geometrical parameters, and is therefore highly dependent on the manipulator's actual configuration.

To further increase a parallel manipulator's accuracy, redundancy can be applied, such that the number of actuators exceeds the number of degrees of freedom (DOFs) of the traveling platform [4]. Two redundancy approaches are established for parallel manipulators, actuation redundancy and kinematic redundancy [5], [6]. Actuation redundancy can be realized whether by adding a kinematic chain to the mechanism or by actuating a passive joint. It leads to internal preload that can be controlled in order to prevent backlash [7]. As a result, the achievable accuracy increases. The drawback of this approach is that such a manipulator cannot be controlled by using a conventional position control scheme [8]. Furthermore, an additional kinematic chain mostly reduces the total workspace [9]. Therefore, in the present paper we focus exclusively on kinematic redundancy, realized by adding at least one actuated joint to one kinematic chain [6], [10].

In [9] we proposed a redundant scheme for the classical 3RRR mechanism. One of the base joints is additionally actuated using a prismatic actuator. The introduced mechanism is denoted by 3(P)RRR. Due to the kinematic redundancy, the inverse displacement problem has an infinite number of solutions [11]. Therefore, the additional redundant DOF can be used to improve several performance indices, e.g the accuracy. This can be done at the task planning stage or while operating the manipulator. Our key idea is to change the position of the redundant actuator in a discrete manner while operating the system, in particular just before shifts in direction of the traveling platform. This allows the reconfiguration of the manipulator to influence its accuracy for a given trajectory segment. We call the resulting set of discrete actuator positions the *switching pattern*. After each switching operation, e.g. after each reconfiguration, the additional prismatic actuator is supposed to remain locked. Therefore, the joint clearance as well as the control error corresponding to the redundant actuator can be minimized. The optimization of the switching patterns is achieved according to a performance index that we call the *gain* of the Jacobian matrix. In comparison to classical performance indices which are related to the accuracy, like the condition number of the Jacobian matrix, the proposed optimization criterion leads to more appropriate solutions concerning the optimized switching patterns.

This paper is organized as follows. In section II the geometric and the inverse kinematic models of the proposed manipulator are given as well as fundamental definitions related to the Jacobian analysis. Section III gives a short theoretical overview on the determination of a traveling platform's accuracy. Furthermore, the optimization strategy developed for the redundant actuator's position is introduced. In section IV several analysis examples are presented in order to validate the proposed redundant scheme with optimized switching patterns. Section V closes the paper with the conclusions.

II. Redundant 3(P)RRR manipulator

In [9] we introduced the kinematically redundant 3(P)RRR planar manipulator presented in Fig. 1. It is basically similar to the non-redundant 3RRR manipulator studied amongst others in [12]. Three kinematic chains $A_iM_iB_i$ $(i = 1, 2, 3)$ connect the moving platform $B_1B_2B_3$ to the base $A_1A_2A_3$. The base-fixed revolute joints are active while the remaining ones are passive. Each kinematic chain consists of two links $l_{i,1}$ and $l_{i,2}$. The added prismatic actuator allows any arbitrary base joint, e.g. A_1, to move linearly. As a result, reconfiguration of the mechanism can be performed selectively while operating the manipulator. The orientation of the redundant actuator with respect to the x-axis of the inertial coordinate frame $(CF)_0$ is denoted by α. Positions referenced with respect to the platform fixed coordinate frame $(CF)_E$ are marked with $(')$.

All authors are with the Institute of Robotics, Leibniz Universität Hannover, Hanover, Germany. kotlarski@ifr.uni-hannover.de

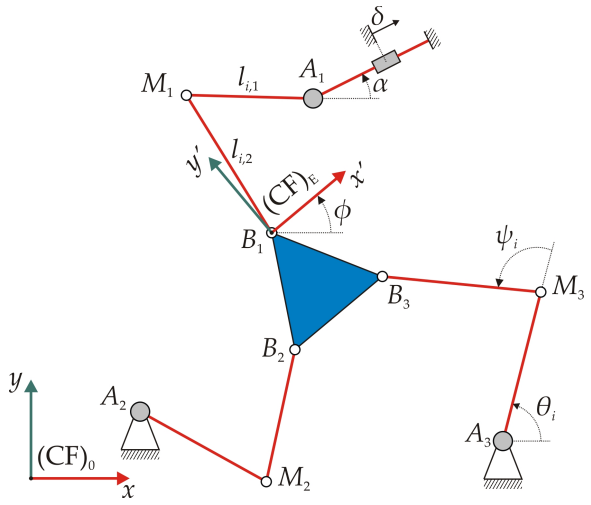

Fig. 1. Kinematically redundant 3(P)RRR manipulator

In the following the configuration of the traveling platform is given by

$$\boldsymbol{x} = [x_{\mathrm{E}},\ y_{\mathrm{E}},\ \phi]^{\mathrm{T}} = [x_{\mathrm{B}_1},\ y_{\mathrm{B}_1},\ \phi]^{\mathrm{T}}, \tag{1}$$

where x_{E} and y_{E} represent the position of $(\mathrm{CF})_{\mathrm{E}}$ with respect to $(\mathrm{CF})_0$ and ϕ is its orientation. The mechanism is driven by the four actuators. Therefore, the system's configuration is given by the according actuator coordinates

$$\boldsymbol{\theta} = [\theta_1,\ \theta_2,\ \theta_3,\ \delta]^{\mathrm{T}}. \tag{2}$$

A. Inverse kinematic

For each kinematic chain i the geometric constraints can be written as

$$x_{\mathrm{B}_i} = x_{\mathrm{A}_i} + l_{i,1}\cos(\theta_i) + l_{i,2}\cos(\theta_i + \psi_i), \tag{3}$$
$$y_{\mathrm{B}_i} = y_{\mathrm{A}_i} + l_{i,1}\sin(\theta_i) + l_{i,2}\sin(\theta_i + \psi_i), \tag{4}$$

where the position of the traveling platform's passive joints with respect to $(\mathrm{CF})_0$ is defined as

$$\begin{bmatrix} x_{\mathrm{B}_i} \\ y_{\mathrm{B}_i} \end{bmatrix} = \begin{bmatrix} x_{\mathrm{E}} \\ y_{\mathrm{E}} \end{bmatrix} + \begin{bmatrix} \cos(\phi) & -\sin(\phi) \\ \sin(\phi) & \cos(\phi) \end{bmatrix} \begin{bmatrix} x'_{\mathrm{B}_i} \\ y'_{\mathrm{B}_i} \end{bmatrix}. \tag{5}$$

In our redundant case the position of A_1 depends on the actuator position δ:

$$\begin{bmatrix} x_{\mathrm{A}_1} \\ y_{\mathrm{A}_1} \end{bmatrix} = \begin{bmatrix} x_{\mathrm{A}_1}(\delta = 0) \\ y_{\mathrm{A}_1}(\delta = 0) \end{bmatrix} + \begin{bmatrix} \delta\cos(\alpha) \\ \delta\sin(\alpha) \end{bmatrix}. \tag{6}$$

From (3) and (4) we can determine the passive joint angles ψ_i:

$$\psi_i = \pm\arccos\left(\frac{x_{\mathrm{AB}_i}^2 + y_{\mathrm{AB}_i}^2 - l_{i,1}^2 - l_{i,2}^2}{2 l_{i,1} l_{i,2}}\right), \tag{7}$$

and finally the active joint angles θ_i:

$$\theta_i = \arctan\left(\frac{(l_{i,1} + l_{i,2}\cos(\psi_i))\, y_{\mathrm{AB}_i} - (l_{i,2}\sin(\psi_i))\, x_{\mathrm{AB}_i}}{(l_{i,1} + l_{i,2}\cos(\psi_i))\, x_{\mathrm{AB}_i} + (l_{i,2}\sin(\psi_i))\, y_{\mathrm{AB}_i}}\right), \tag{8}$$

where $x_{\mathrm{AB}_i} = x_{\mathrm{B}_i} - x_{\mathrm{A}_i}$ and $y_{\mathrm{AB}_i} = y_{\mathrm{B}_i} - y_{\mathrm{A}_i}$.

B. Jacobian formulation

After summing the squares of (3) and (4) the manipulator's Jacobian matrix $\boldsymbol{J}$ can be obtained by a derivation with respect to time [13]:

$$\boldsymbol{A}\dot{\boldsymbol{x}} = \boldsymbol{B}\dot{\boldsymbol{\theta}} \ \Leftrightarrow\ \dot{\boldsymbol{x}} = \boldsymbol{A}^{-1}\boldsymbol{B}\dot{\boldsymbol{\theta}} = \boldsymbol{J}\dot{\boldsymbol{\theta}}. \tag{9}$$

For the here considered manipulator the direct and inverse Jacobian matrices $\boldsymbol{A}$ and $\boldsymbol{B}$ result to

$$\boldsymbol{A} = \begin{bmatrix} a_{11} & a_{12} & a_{13} \\ a_{21} & a_{22} & a_{23} \\ a_{31} & a_{32} & a_{33} \end{bmatrix},\ \boldsymbol{B} = \begin{bmatrix} b_{11} & 0 & 0 & b_{14} \\ 0 & b_{22} & 0 & 0 \\ 0 & 0 & b_{33} & 0 \end{bmatrix}, \tag{10}$$

with (for $i = 1, 2, 3$)

$$\begin{aligned} a_{i1} &= x_{\mathrm{B}_i} - x_{\mathrm{A}_i} - l_{i,1}\cos\theta_i, \\ a_{i2} &= y_{\mathrm{B}_i} - y_{\mathrm{A}_i} - l_{i,1}\sin\theta_i, \\ a_{i3} &= -a_{i1}\left(x'_{\mathrm{B}_i}\sin(\phi) + y'_{\mathrm{B}_i}\cos(\phi)\right) \\ &\quad + a_{i2}\left(x'_{\mathrm{B}_i}\cos(\phi) - y'_{\mathrm{B}_i}\sin(\phi)\right), \end{aligned} \tag{11}$$

and

$$\begin{aligned} b_{ii} &= l_{i,1}\left(a_{i1}\sin(\theta_i) - a_{i2}\cos(\theta_i)\right), \\ b_{14} &= -\left(a_{11}\cos(\alpha) + a_{12}\sin(\alpha)\right). \end{aligned} \tag{12}$$

III. Accuracy Improvement using Kinematic Redundancy

In the following the theoretical background of the determination of a traveling platform's accuracy is outlined. Furthermore, the developed optimization strategy concerning the improvement of the pose accuracy is introduced.

A. The traveling platform's pose error

Due to several factors, like manufacturing errors, joint clearance, and active joint errors, the pose of a traveling platform can be provided within a given accuracy only. Referring to [14], the active joint errors, e.g. the limited resolution of the encoders, are the major sources of error in a calibrated and precisely manufactured parallel manipulator. Therefore, we focus our analysis on the achievable accuracy of a traveling platform in the presence of active joint errors only.

By rewriting the velocity equation (9) in incremental form, we obtain an approximation that maps the active joint errors (the input error) $\Delta\boldsymbol{\theta}$ to the pose error (the output error) $\Delta\boldsymbol{x}$:

$$\Delta\boldsymbol{x} = \boldsymbol{J}(\boldsymbol{\xi}, \boldsymbol{x}, \delta)\Delta\boldsymbol{\theta}, \tag{13}$$

where $\boldsymbol{\xi}$ contains the geometric parameters of the robot. The vector $\boldsymbol{x}$ is the traveling platform's configuration and δ is the position of the redundant actuator. Using (13) and incorporating the fact that $|ab| = |a||b|$ and $|a+b| \leq |a|+|b|$ $\forall\ (a, b) \in \mathbb{R}$ the maximal pose error vector $\overline{\Delta\boldsymbol{x}}$ can be calculated by

$$\begin{bmatrix} \overline{\Delta x} \\ \overline{\Delta y} \\ \overline{\Delta\phi} \end{bmatrix} = \begin{bmatrix} |J_{11}| & |J_{12}| & |J_{13}| & |J_{14}| \\ |J_{21}| & |J_{22}| & |J_{23}| & |J_{24}| \\ |J_{31}| & |J_{32}| & |J_{33}| & |J_{34}| \end{bmatrix} \begin{bmatrix} |\Delta\theta_1| \\ |\Delta\theta_2| \\ |\Delta\theta_3| \\ |\Delta\delta| \end{bmatrix}. \tag{14}$$

Here, J_{ij} is the Jacobian's element of row i and column j. Since the Jacobian matrix $\boldsymbol{J}$ depends on the actuator position δ, the additional DOF of the proposed kinematically redundant manipulator can be used to affect the Jacobian's elements and therefore the robot's accuracy directly. Fig. 2 shows the elements of $\overline{\Delta \boldsymbol{x}}$ with respect to the actuator position δ for an exemplary redundant manipulator with an arbitrarily chosen active joint error $\Delta\boldsymbol{\theta}$. The dependency

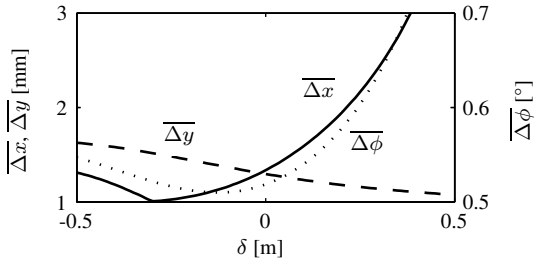

Fig. 2. Positioning error $\overline{\Delta \boldsymbol{x}}$ with respect to the actuator position δ and for a constant pose $\boldsymbol{x}$

of the achievable accuracy on the actuator position δ is well noticeable. But, the components of the maximal pose error $\overline{\Delta x}$, $\overline{\Delta y}$, and $\overline{\Delta \phi}$ have individual minima with respect to different actuator positions. Therefore, an optimization procedure is required in order to find the most appropriate solution for δ.

B. Optimization of the actuator position δ

The optimization of the redundant actuator position δ can be performed based on two strategies: A classical continuous optimization and a selective discrete optimization. The latter is the key idea of the present paper and is discussed in the following.

Undoubtedly, a continuous optimization leads to an instantly influenceable accuracy. In contrast to the mentioned advantage, it results in a more challenging task concerning the robot's control and often in a higher energy demand. Our approach is based on the optimization of the actuator position δ in a discrete manner while operating the system. Therefore, the trajectory to be executed is divided into segments. The start and end points of the segments are certain poses, i.e. shifts in direction. Appropriate constant values of the actuator position δ corresponding to the different segments of the desired trajectory are determined. The resulting set of discrete actuator positions is called the optimized *switching pattern*. While moving along the desired trajectory, the position of the redundant actuator δ is changed according to the switching pattern. This allows the reconfiguration of the manipulator to influence its accuracy for a given path segment. While performing a reconfiguration the traveling platform's pose is kept constant. After each switching operation, e.g. while moving along a trajectory segment, the additional prismatic actuator is supposed to remain locked. Therefore, the joint clearance as well as the control error corresponding to the redundant actuator are minimized.

The optimization can be realized with respect to several criteria and performance indices. A well accepted criterion is the condition number (in general the two-norm condition number) of the Jacobian matrix $\kappa(\boldsymbol{J})$ and its inverse $\eta = \kappa^{-1}$ called dexterity. In [15] it is defined as:

$$\kappa = \|J^{-1}\|_2 \|J\|_2, \qquad 1 \leq \kappa \leq \infty, \tag{15}$$

where $\kappa = 1$ represents an isotropic configuration without an amplification of the active joint error $\Delta\boldsymbol{\theta}$ and $\kappa = \infty$ represents a singular configuration with an infinite amplification of $\Delta\boldsymbol{\theta}$. However, the Jacobian matrix $\boldsymbol{J}$ is not homogeneous in terms of physical units. Therefore, the value of the condition number depends on the unit choice. Hence, a modification of the Jacobian matrix is required in order to obtain significant values for κ. Amongst others, the homogeneity can be achieved by transforming the traveling platform's velocity $\dot{\boldsymbol{x}}$ into the linear velocity $\dot{\boldsymbol{x}}^\star = [\dot{x}_{\mathrm{P}_1} \;\; \dot{y}_{\mathrm{P}_1} \;\; \dot{x}_{\mathrm{P}_2} \;\; \dot{y}_{\mathrm{P}_2}]^{\mathrm{T}}$ of two arbitrary points P_1 and P_2 [16]. Therefore, a transformation matrix $\boldsymbol{R}$ has to be found that satisfies the following equation:

$$\dot{\boldsymbol{x}}^\star = \boldsymbol{R}\dot{\boldsymbol{x}}. \tag{16}$$

But, instead of describing a manipulator with three DOFs by four parameters $\dot{\boldsymbol{x}}^\star$, a reduction of the terms describing the velocities of the traveling platform to three can be performed [15]. As a result, the dimension of the Jacobian matrix $\boldsymbol{J}$ remains constant. For the proposed manipulator, the modified transformation matrix $\boldsymbol{R}$ results to:

$$\boldsymbol{R} = \begin{bmatrix} \cos\beta & \sin\beta & 0 \\ -\sin\beta & \cos\beta & 0 \\ -\sin\beta & \cos\beta & x'_{\mathrm{B}_3}\cos\phi - y'_{\mathrm{B}_3}\sin\phi \end{bmatrix}. \tag{17}$$

The angle β gives the orientation of $(\mathrm{CF})_0$ to a coordinate frame located in B_1 with its x-axis passing through B_3. The homogenized Jacobian matrix $\boldsymbol{J}'$ can be determined using the following equation:

$$\boldsymbol{J}' = \boldsymbol{R}\boldsymbol{J}. \tag{18}$$

Hence, an optimization of the actuator position δ can be performed by a minimization of the condition number $\kappa(\boldsymbol{J}')$ and by a maximization of the dexterity $\eta(\boldsymbol{J}')$, respectively:

$$\min_{\delta} \kappa(\boldsymbol{J}') \quad \hat{=} \quad \max_{\delta} \eta(\boldsymbol{J}'). \tag{19}$$

As demonstrated by Merlet [17] and shown later in section IV the condition number does not necessarily exhibit a complete consistent behavior with respect to the pose error of a robot. Therefore, we propose an optimization of the actuator position δ based on minimizing the sums of the absolute values of the elements of the Jacobian's rows. We call this index the *gain* $\gamma(\boldsymbol{J}')$ of the homogenized Jacobian matrix $\boldsymbol{J}'$. Since the influence of the prismatic actuator's joint error on the pose error is small only (see section IV) the last column of the Jacobian matrix is not taken into account. Therefore, the cost function to be minimized results to:

$$\min_{\delta} \gamma(\boldsymbol{J}') = \min_{\delta} \left\| \left| \sum_{i=1}^{3} |J'_{1,i}| \quad \sum_{i=1}^{3} |J'_{2,i}| \quad \sum_{i=1}^{3} |J'_{3,i}| \right| \right\|_2 \tag{20}$$

IV. Accuracy analysis

Several analysis examples are presented in order to validate the proposed redundant scheme with the developed optimized switching patterns. The advantage of our approach is verified for different trajectories. Additionally, it is demonstrated that the active joint error of the redundant prismatic actuator influences marginally the traveling platform's pose accuracy.

In the following, we combine the two translational position errors Δx and Δy of the traveling platform to obtain a quantity for the maximal translational error:

$$\overline{\Delta xy} = \sqrt{\overline{\Delta x}^2 + \overline{\Delta y}^2} \tag{21}$$

A. Simulation of single trajectories

Accuracy analysis along selected simulated trajectories were performed. The geometric parameters $\boldsymbol{\xi}$ of the analyzed kinematic structure are given in TABLE I. Keeping the design space in mind the orientation of the redundant actuator was set to $\alpha = 0°$. Exemplarily, simulation results of

TABLE I

Design parameters $\boldsymbol{\xi}$ of the regarded non-redundant 3RRR and the redundant 3(P)RRR ($-0.5\,\mathrm{m} \leq \delta \leq 0.5\,\mathrm{m}$) manipulator

	$i=1$	$i=2$	$i=3$
$x_{\mathrm{A}_i}\,[m]$	0.6	0	1.2
$y_{\mathrm{A}_i}\,[m]$	$\sqrt{27}/5$	0	0
$x'_{\mathrm{B}_i}\,[m]$	0	-0.1	0.1
$y'_{\mathrm{B}_i}\,[m]$	0	$-\sqrt{3}/10$	$-\sqrt{3}/10$
$l_{i,1}\,[m]$	0.6	0.6	0.6
$l_{i,2}\,[m]$	0.6	0.6	0.6

the three triangular trajectories (I, II, III) shown in Fig. 3 are presented. They were chosen within the manipulator's workspace (dashed black line) such that the non-redundant 3RRR manipulator does not pass any singular poses when $\phi = 0°$. The traveling platform was moved clockwise

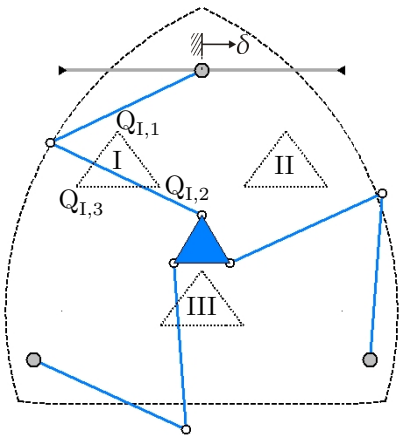

Fig. 3. Intuitively chosen trajectories (I, II, III)

along the chosen trajectories with a constant orientation. The trajectories were divided such that each side of a triangular represents a segment. Hence, at every corner $\mathrm{Q}_{j,1}$, $\mathrm{Q}_{j,2}$, and $\mathrm{Q}_{j,3}$ (j = I,II,III) the position of the redundant actuator δ is switched according to the optimized switching pattern. During each switching operation the traveling platform's pose is kept constant. The optimization was performed based on the introduced cost functions (19) and (20). Even though the prismatic joint is locked between two switching phases, its joint error, e.g. the limited resolution of the encoder, has to be taken into account in order to obtain a significant accuracy analysis. Therefore, the active joint errors were chosen based on data sheets of commercially available standard actuators to $\Delta\boldsymbol{\theta} = [0.1° \; 0.1° \; 0.1° \; 10\,\mu\mathrm{m}]^{\mathrm{T}}$.

In Fig. 4 the optimized switching patterns of the actuator position δ as well as the resulting manipulator's pose errors $\overline{\Delta xy}$ and $\overline{\Delta\phi}$ are presented. The traveling platform was moved along trajectory I with a constant orientation of $\phi = 0°$ denoted as I($0°$). A significant improvement of the

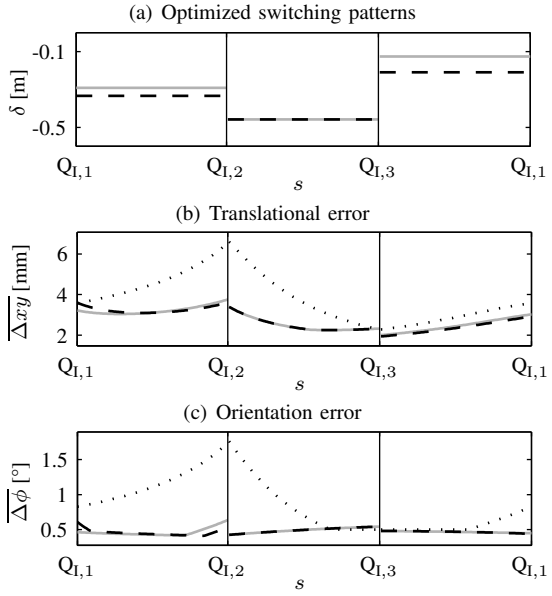

Fig. 4. Simulation results while moving along trajectory I($0°$) (dotted black: Non-redundant manipulator; dashed black: Optimized redundant manipulator using $\eta(\boldsymbol{J}')$; solid gray: Optimized redundant manipulator using $\gamma(\boldsymbol{J}')$

accuracy due to the kinematic redundancy is well noticeable. The maximal pose error occurring close to $\mathrm{Q}_{\mathrm{I},2}$ was minimized by a reconfiguration of the manipulator according to the optimized switching pattern. Fig. 4 shows that both optimization criteria lead to similar switching patterns and to similar achievable accuracies. But, later simulation results (see section IV-B) will clarify the advantage of the developed optimization based on the gain $\gamma(\boldsymbol{J}')$.

In order to quantify the accuracy improvement we determine the maximal translational $\overline{\Delta xy}_{\max}$ and rotational error $\overline{\Delta\phi}_{\max}$ of the traveling platform over a complete trajectory. The values represent the achievable accuracy of the associated manipulator. An overview of the maximal errors of the three triangular trajectories shown in Fig. 3 are given in TABLE II. Additionally, the percentage improvements of

the kinematically redundant manipulator in comparison to its non-redundant counterpart are given. Taking a look at

TABLE II

MAXIMAL TRANSLATIONAL $\overline{\Delta xy}_{\max}$ AND ROTATIONAL ERROR $\overline{\Delta\phi}_{\max}$ OF THE TRAVELING PLATFORM WHILE MOVING ALONG TRAJECTORY I, II, AND III

$j(\phi)$	Value	3RRR	3(P)RRR	
			using $\eta(\boldsymbol{J}')$	using $\gamma(\boldsymbol{J}')$
I($-45°$)	$\overline{\Delta xy}_{\max}$ [mm]	764.77	10.30 (99.7%)	6.57 (99.8%)
	$\overline{\Delta\phi}_{\max}$ [°]	2954.45	1.07 (99.9%)	1.26 (99.8%)
I(0°)	$\overline{\Delta xy}_{\max}$ [mm]	6.60	3.61 (45.4%)	3.76 (43.0%)
	$\overline{\Delta\phi}_{\max}$ [°]	1.76	0.61 (65.4%)	0.64 (63.7%)
I(45°)	$\overline{\Delta xy}_{\max}$ [mm]	6.34	3.60 (43.3%)	3.85 (39.4%)
	$\overline{\Delta\phi}_{\max}$ [°]	7.02	5.46 (22.3%)	5.34 (24.0%)
II($-45°$)	$\overline{\Delta xy}_{\max}$ [mm]	54.01	2.42 (95.5%)	2.26 (95.8%)
	$\overline{\Delta\phi}_{\max}$ [°]	11.10	0.50 (95.5%)	0.47 (95.8%)
II(0°)	$\overline{\Delta xy}_{\max}$ [mm]	4.98	2.14 (57.0%)	2.02 (59.4%)
	$\overline{\Delta\phi}_{\max}$ [°]	2.23	0.81 (63.8%)	0.75 (66.3%)
II(45°)	$\overline{\Delta xy}_{\max}$ [mm]	6.01	4.52 (24.7%)	3.87 (35.6%)
	$\overline{\Delta\phi}_{\max}$ [°]	2.62	1.77 (32.5%)	1.71 (34.9%)
III($-45°$)	$\overline{\Delta xy}_{\max}$ [mm]	2.34	3.49 (-49.0%)	1.92 (17.8%)
	$\overline{\Delta\phi}_{\max}$ [°]	0.61	0.65 (-7.1%)	0.60 (0.7%)
III(0°)	$\overline{\Delta xy}_{\max}$ [mm]	2.35	2.38 (-1.3%)	2.03 (13.4%)
	$\overline{\Delta\phi}_{\max}$ [°]	1.06	1.09 (-2.1%)	1.02 (4.2%)
III(45°)	$\overline{\Delta xy}_{\max}$ [mm]	16.27	28.22 (-73.4%)	15.68 (3.7%)
	$\overline{\Delta\phi}_{\max}$ [°]	5.06	8.41 (-66.1%)	5.17 (-2.2%)

the results of trajectory I and II, both optimization criteria ($\eta(\boldsymbol{J}')$ and $\gamma(\boldsymbol{J}')$) lead to an improvement of the achievable accuracy. Attention should be paid to I($-45°$). Here, the non-redundant manipulator passes through a singularity. As a result, its pose error increases highly. In case of the proposed kinematically redundant manipulator and an optimization of its configuration the singularity, i.e. the large pose error, was avoided.

Focussing on the results obtained while moving along trajectory III, the advantage of the proposed optimization based on the Jacobian's gain $\gamma(\boldsymbol{J}')$ is noticeable. Using $\eta(\boldsymbol{J}')$ caused a decrease of the achievable accuracy in all cases. This is a practical proof (further confirmed in section IV-B) of what we claimed in section III and noticed in [17]: The condition number does not necessarily exhibit a complete consistent behavior with respect to the pose error of a robot.

An additional test was performed to demonstrate the marginal influence of the prismatic actuator's joint error on the traveling platform's pose error. Therefore, for different $\Delta\delta$ the traveling platform was moved along I(0°). The actuator position δ was changed according to the optimized switching pattern shown in Fig. 4 (based on the Jacobian's gain). The results are presented in Fig. 5. The plots clearly demonstrate the marginal influence of $\Delta\delta$ on the traveling platform's pose error $\Delta\boldsymbol{x}$.

B. Complex testing scenario

In order to further confirm the results obtained in section IV-A we developed a complex testing scenario. Several different trajectories were considered. For different orientations $-90° \leq \phi \leq 90°$ the traveling platform was moved

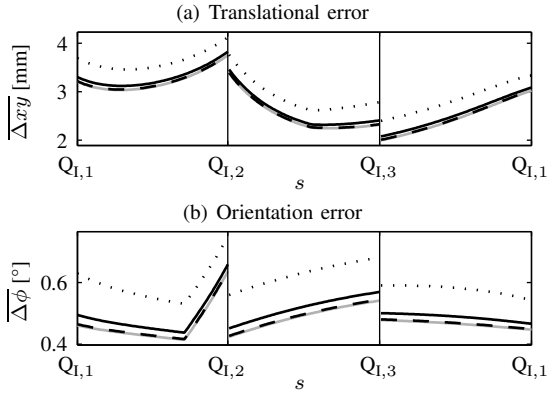

Fig. 5. Influence of the prismatic joint error $\Delta\delta$ on the traveling platform's pose error while moving along trajectory I(0°) (solid gray: $\Delta\delta = 0$; dashed black: $\Delta\delta = 10\,\mu$m; solid black: $\Delta\delta = 100\,\mu$m; dotted black: $\Delta\delta = 500\,\mu$m

along generated trajectories exemplarily shown for $\phi = 0°$ in Fig. 6. The triangular and rectangular trajectories were

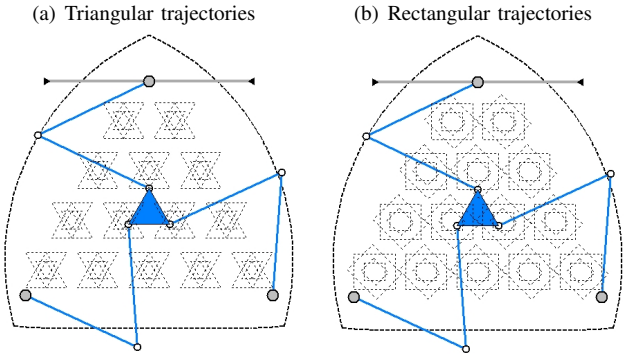

Fig. 6. Exemplary trajectories of the complex testing scenario

located all over the workspace. Again, each trajectory was divided such that each side of a triangular and rectangular represents a segment. The overall joint error was set to $\Delta\boldsymbol{\theta} = [0.1° \; 0.1° \; 0.1° \; 10\,\mu\text{m}]^{\text{T}}$ and the maximal pose error $\overline{\Delta\boldsymbol{x}}$ was determined using (14). It is important to notice that the optimization was achieved using nominal values of $\boldsymbol{\xi}$, whereas the simulation was carried out under mistuned values, in order to meet the realistic case. The results of the testing scenario regarding the geometric parameter $\boldsymbol{\xi}$ are summarized in TABLE III and are given graphically in Fig. 7. The means μ as well as the standard deviations σ of the

TABLE III

SIMULATION RESULTS OF THE TESTING SCENARIO (OVERALL VALUES TAKING ALL ANALYZED ORIENTATIONS INTO ACCOUNT)

Value	3RRR	3(P)RRR	
		using $\eta(\boldsymbol{J}')$	using $\gamma(\boldsymbol{J}')$
$\mu(\overline{\Delta xy})$ [mm]	8.13	9.56 (-17.7%)	2.73 (66.3%)
$\mu(\overline{\Delta\phi})$ [°]	2.53	3.13 (-24.0%)	0.94 (62.9%)
$\sigma(\overline{\Delta xy})$ [mm]	74.75	236.91 (-217.0%)	3.6 (95.20%)
$\sigma(\overline{\Delta\phi})$ [°]	23.82	71.03 (-198.1%)	1.32 (94.5%)

traveling platform's maximal errors $\overline{\Delta xy}$ and $\overline{\Delta\phi}$ are shown.

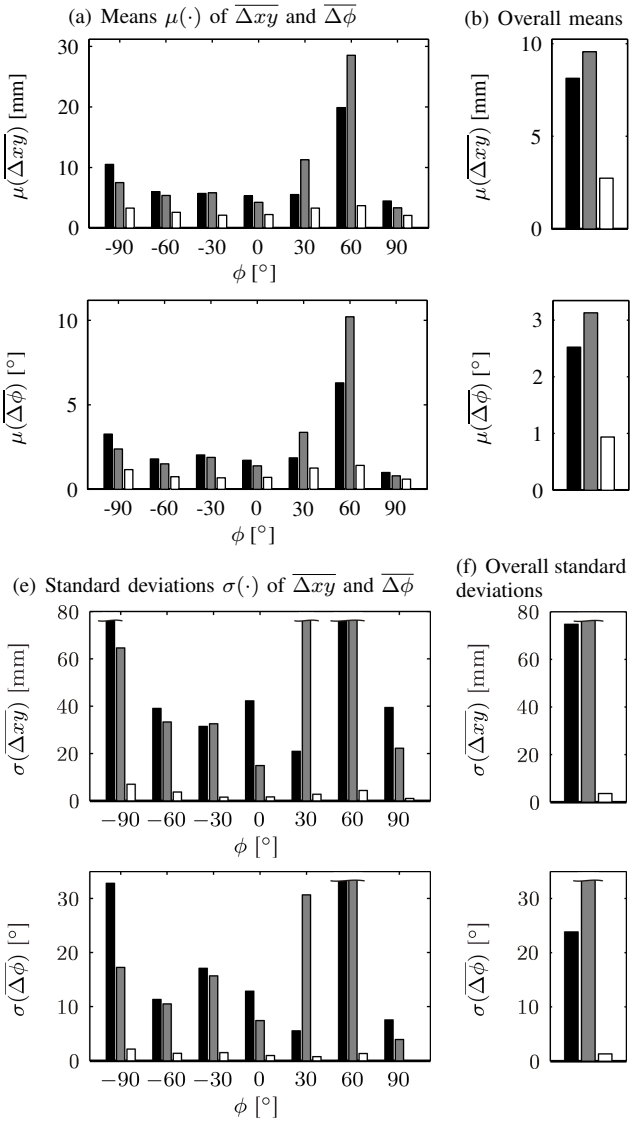

Fig. 7. Simulation results of the testing scenario of the robot defined with $\boldsymbol{\xi}$ (black: Non-redundant manipulator; gray: Optimized redundant manipulator using $\eta(\boldsymbol{J}')$; white: Optimized redundant manipulator using $\gamma(\boldsymbol{J}')$)

Often, inappropriate switching patterns were obtained when the actuator position δ was optimized based on the dexterity $\eta(\boldsymbol{J}')$. Especially, the results of $\phi = 30°$ and $\phi = 60°$ demonstrate the inconsistency of the condition number with respect to the accuracy. In contrast, the developed optimization based on the gain $\gamma(\boldsymbol{J}')$ leads to an improvement of the accuracy as well as of the precision in all cases. Optimizing the actuator position δ using the proposed Jacobian's gain $\gamma(\boldsymbol{J}')$ led to consistent improvements of the manipulator's accuracy greater than 90%.

V. Conclusions

In this paper, a kinematically redundant 3(P)RRR mechanism was presented. After a description of some fundamentals of the proposed manipulator, the effect of the additional DOF on the traveling platform's accuracy was clarified. An optimization of the redundant actuator's position in a discrete manner was developed. It is based on a minimization of a criterion that we denoted the *gain* $\gamma(\boldsymbol{J}')$ of the homogenized Jacobian matrix $\boldsymbol{J}'$. We showed that the proposed index leads to more appropriate *switching patterns* than the Jacobian's condition number. Several analysis examples demonstrate a great improvement in terms of accuracy and precision of the proposed redundant manipulator in combination with the developed optimization procedure.

Future work will deal with the experimental validation of the obtained simulation results.

References

[1] H. S. Kim and Y. J. Choi, "The kinematic error bound analysis of the stewart platform," *Journal of Robotic Systems*, vol. 17, no. 1, pp. 63–73, October 2000.

[2] J.-P. Merlet, "Jacobian, manipulability, condition number, and accuracy of parallel robots," *Journal of Mechanical Design*, vol. 128, no. 1, pp. 199–206, January 2006.

[3] J.-P. Merlet and D. Daney, "Dimensional synthesis of parallel robots with a guaranteed given accuracy over a specific workspace," in *2005 IEEE International Conference on Robotics and Automation*, April 2005, pp. 942–947.

[4] J.-P. Merlet, "Redundant parallel manipulators," *Laboratory Robotics and Automation*, vol. 8, no. 1, pp. 17–24, February 1996.

[5] S. Kock and W. Schumacher, "A parallel x-y manipulator with actuation redundancy for high-speed and active-stiffness applications," in *1998 IEEE International Conference on Robotics and Automation*, May 1998, pp. 2295–2300.

[6] J. Wang and C. M. Gosselin, "Kinematic analysis and design of kinematically redundant parallel mechanisms," *Journal of Mechanical Design*, vol. 126, no. 1, pp. 109–118, January 2004.

[7] A. Müller, "Internal preload control of redundantly actuated parallel manipulators & its application to backlash avoiding control," *IEEE Transactions on Robotics and Automation*, vol. 21, no. 4, pp. 668–677, August 2005.

[8] S. Kock, "Parallelroboter mit Antriebsredundanz," Ph.D. dissertation, Institute of Control Engineering, TU Brunswick, Germany, March 2001.

[9] J. Kotlarski, H. Abdellatif, and B. Heimann, "On singularity avoidance and workspace enlargement of planar parallel manipulators using kinematic redundancy," in *13th IASTED International Conference on Robotics and Applications*, August 2007.

[10] S.-H. Cha, T. A. Lasky, and S. A. Velinsky, "Singularity avoidance for the 3-RRR mechanism using kinematic redundancy," in *2007 IEEE International Conference on Robotics and Automation*, April 2007, pp. 1195–1200.

[11] I. Ebrahimi, J. A. Carretero, and R. Boudreau, "3-PRRR redundant planar parallel manipulator: Inverse displacement, workspace and singularity analyses," *Mechanism & Machine Theory*, vol. 42, no. 8, pp. 1007–1016, August 2007.

[12] M. Arsenault and R. Boudreau, "Synthesis of planar parallel mechanisms while considering workspace, dexterity, stiffness and singularity avoidance," *Journal of Mechanical Design*, vol. 128, pp. 69–78, January 2006.

[13] C. M. Gosselin and J. Angeles, "Singularity analysis of closed-loop kinematic chains," *IEEE Transactions on Robotics and Automation*, vol. 6, no. 3, pp. 281–290, June 1990.

[14] J.-P. Merlet, "Computing the worst case accuracy of a pkm over a workspace or a trajectory," in *The 5th Chemnitz Parallel Kinematics Seminar*, April 2006, pp. 83–96.

[15] C. M. Gosselin, "Optimum design of robotic manipulators using dexterity indices," *Robotics and Autonomous Systems*, vol. 9, no. 4, pp. 213–226, 1992.

[16] G. Pond and J. A. Carretero, "Formulating jacobian matrices for the dexterity analysis of parallel manipulators," *Mechanism & Machine Theory*, vol. 41, no. 12, pp. 1505–1519, December 2006.

[17] J.-P. Merlet, *Parallel Robots (Second Edition)*. Dordrecht: Springer, 2006.